

**Targeting the Metastasis Suppressor, NDRG1, Using Novel Iron Chelators:
Regulation of Stress Fiber-Mediated Tumor Cell Migration *via* Modulation of the
ROCK1/pMLC2 Signaling Pathway**

**Jing Sun , Daohai Zhang , Ying Zheng, Qian Zhao, Minhua Zheng , Zaklina
Kovacevic and Des R. Richardson**

Molecular Pharmacology

Supplementary Data

Supplementary Figure 1. Wound-healing assays confirm the effect of NDRG1 expression on inhibiting the migration of DU145, HT29 and HCT116 cells.

Supplementary Figure 2. Co-localization of pMLC2 together with F-actin, forming stress fibers after NDRG1 was knocked down in: (A) DU145, (B) HT29 and (C) HCT116 cells.

Supplementary Figure 3. The ROCK1 inhibitor, Y27632, inhibits MLC2 phosphorylation and stress fiber formation in DU145, HT29, and HCT116 cells.

Supplementary Figure 4. Iron chelators inhibit stress fiber assembly and MLC2 phosphorylation in DU145 cells.

Supplementary Figure 5. Iron chelators inhibit stress fiber assembly and MLC2 phosphorylation in HT29 cells.

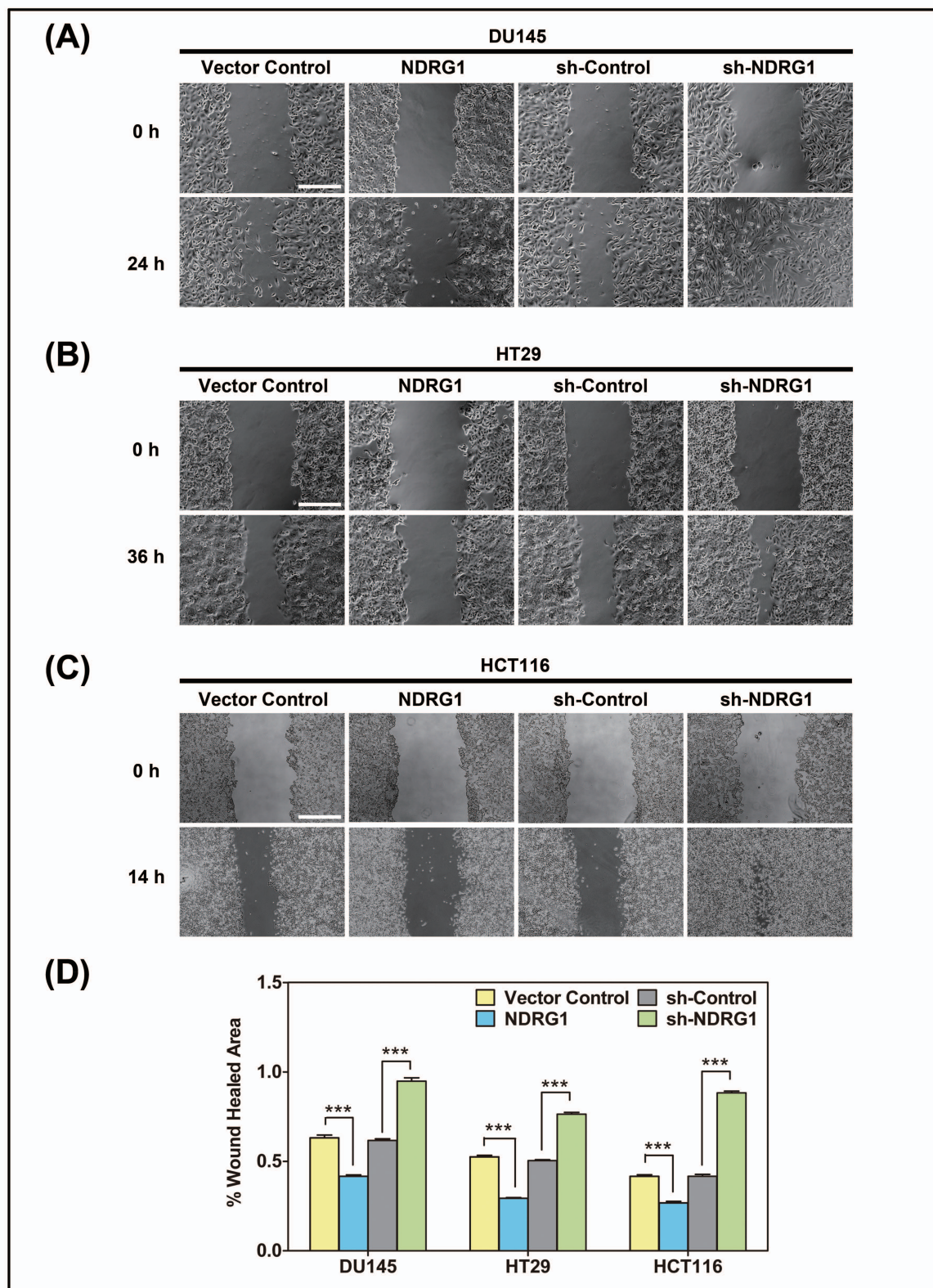
Supplementary Figure 6. Iron chelators inhibit stress fiber assembly and MLC2 phosphorylation in HCT116 cells.

Targeting the Metastasis Suppressor, NDRG1, Using Novel Iron Chelators: Regulation of Stress Fiber-Mediated Tumor Cell Migration via Modulation of the ROCK1/pMLC2 Signaling Pathway

Jing Sun , Daohai Zhang , Ying Zheng, Qian Zhao, Minhua Zheng , Zaklina Kovacevic and Des R. Richardson

Molecular Pharmacology

Supplementary Figure 1



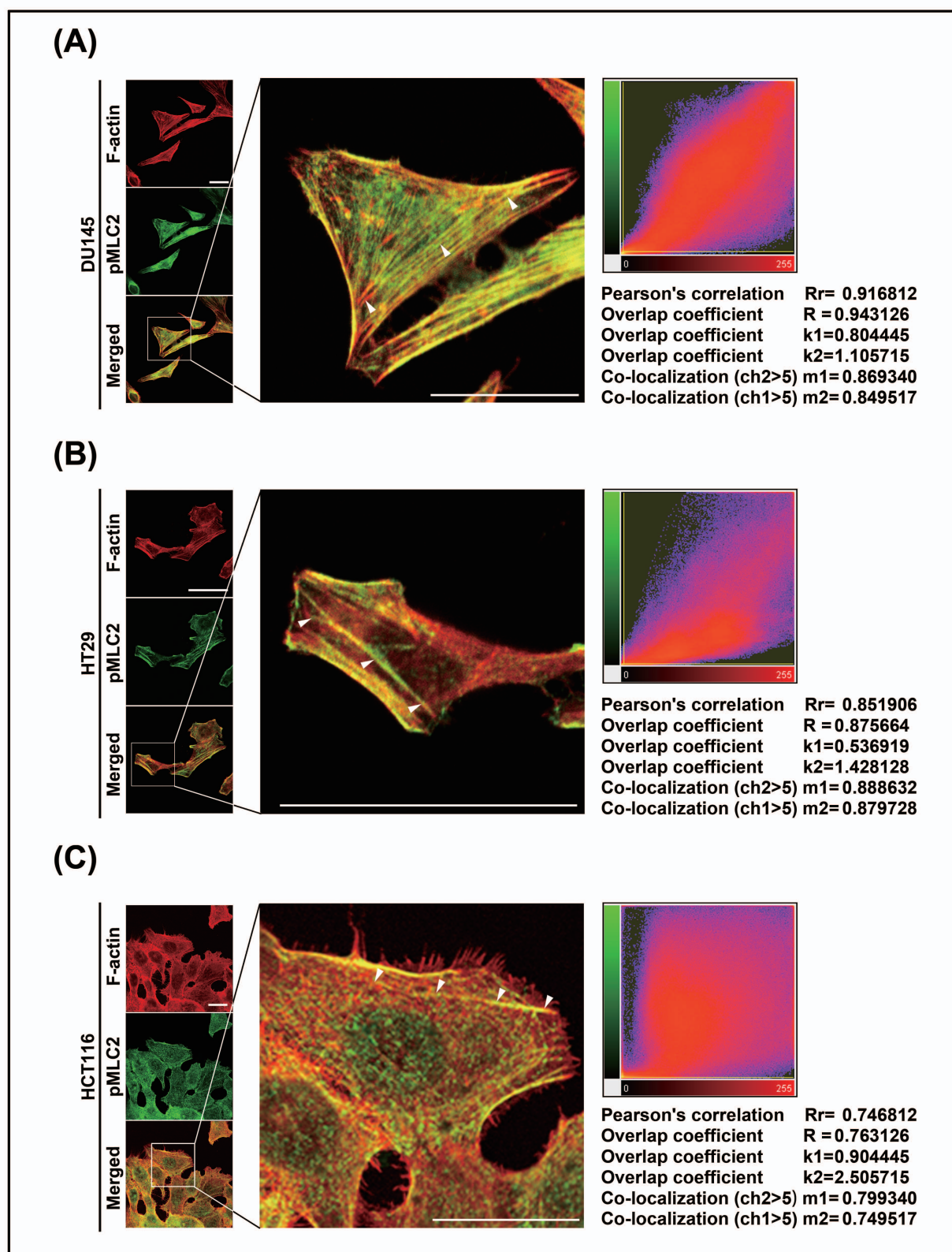
Supplementary Figure 1. Wound-healing assays confirm the effect of NDRG1 expression on inhibiting the migration of DU145, HT29 and HCT116 cells. (A-C) The DU145, HT29 and HCT116 NDRG1 over-expression and knockdown clones, as well as relative control cells (Vector Control and sh-Control), were seeded into 12-well plates (2% gelatin coated) until they reached confluence. A wound was then created by manually scraping the cell monolayer with a Gilson p200 pipette tip. Images were acquired using an Olympus IX50 inverted microscope (Olympus, Tokyo, Japan) with a 10× objective at: (A) 0 h and 24 h (DU145 cells); (B) 0 h and 36 h (HT29 cells) and (C) 0 h and 14 h (HCT116 cells). The migrated area was quantitated using the program Image J to analyze cell migration ability. Scale bar: 1 mm. (D) Quantitative analysis of cell migration ability after NDRG1 over-expression and knockdown was performed by comparing the wound area that cells migrated into from the starting point (0 h) to the end point (24 h for DU145 cells, 36 h for HT29 cells and 14 h for HCT116 cells). Results are typical of 3-5 images from different visual fields and the histogram values are mean ± SD (3-5 images). *** $p < 0.001$, relative to Vector Control or sh-Control cells.

Targeting the Metastasis Suppressor, NDRG1, Using Novel Iron Chelators: Regulation of Stress Fiber-Mediated Tumor Cell Migration via Modulation of the ROCK1/pMLC2 Signaling Pathway

Jing Sun , Daohai Zhang , Ying Zheng, Qian Zhao, Minhua Zheng , Zaklina Kovacevic and Des R. Richardson

Molecular Pharmacology

Supplementary Figure 2



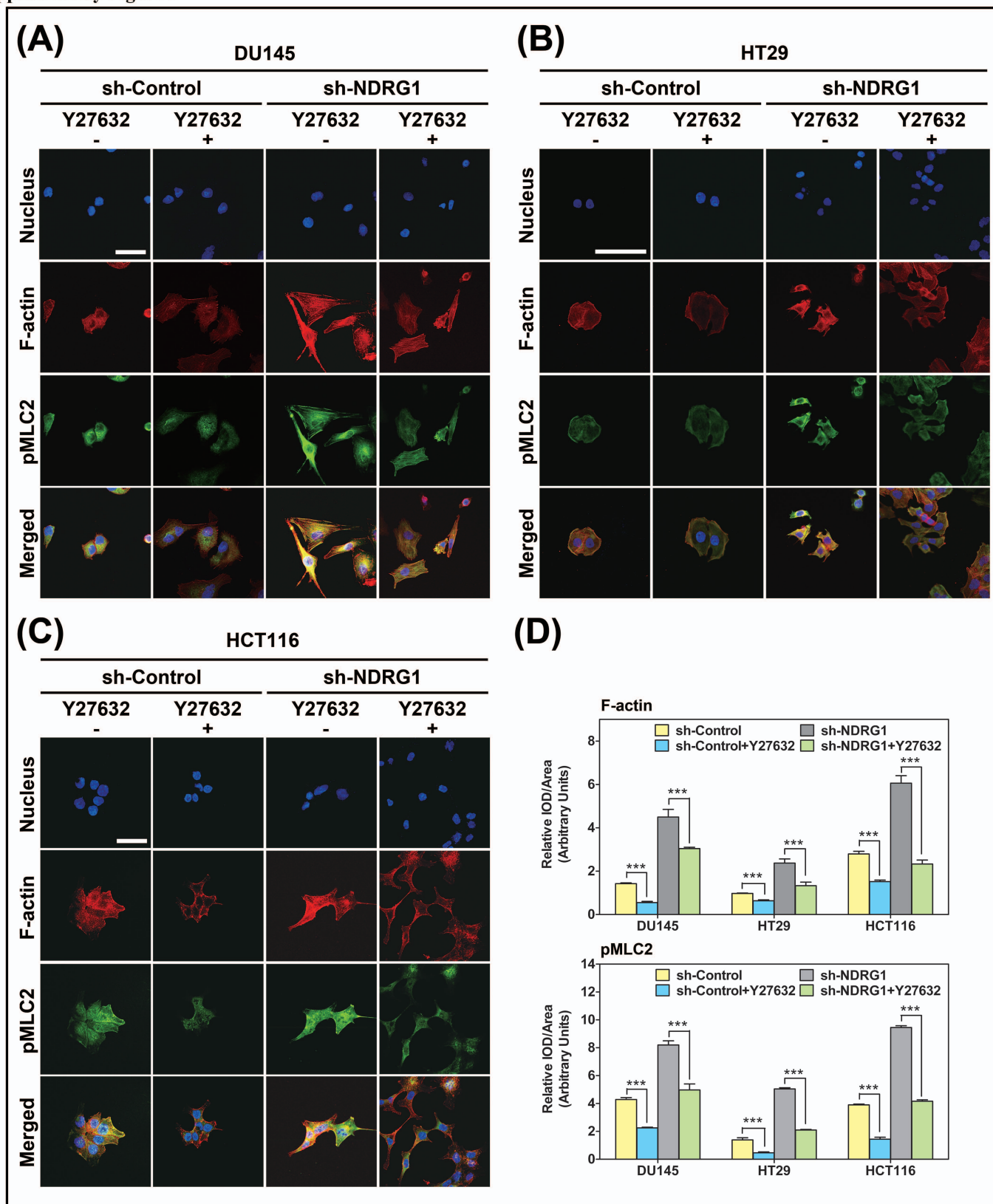
Supplementary Figure 2. Co-localization of pMLC2 together with F-actin, forming stress fibers after NDRG1 was knocked down in: (A) DU145, (B) HT29 and (C) HCT116 cells. Merged immunofluorescence images from Fig. 5A-C in the main text were enlarged to show F-actin (red) stained with rhodamine phalloidin and pMLC2 (green) stained with Alexa Fluor® 488 in NDRG1-knockdown DU145, HT29 and HCT116 cells. There were high correlation coefficients (Pearson's correlation: 0.75-0.92) between F-actin and pMLC2 in all three cell-types, indicating pMLC2 co-localized together with F-actin, forming filament bundles when NDRG1 was knocked down. White arrows indicate stress fibers. Scale bar: 25 μ m. Co-localization analysis was performed using the program, Imaris 7.3.

Targeting the Metastasis Suppressor, NDRG1, Using Novel Iron Chelators: Regulation of Stress Fiber-Mediated Tumor Cell Migration via Modulation of the ROCK1/pMLC2 Signaling Pathway

Jing Sun , Daohai Zhang , Ying Zheng, Qian Zhao, Minhua Zheng , Zaklina Kovacevic and Des R. Richardson

Molecular Pharmacology

Supplementary Figure 3



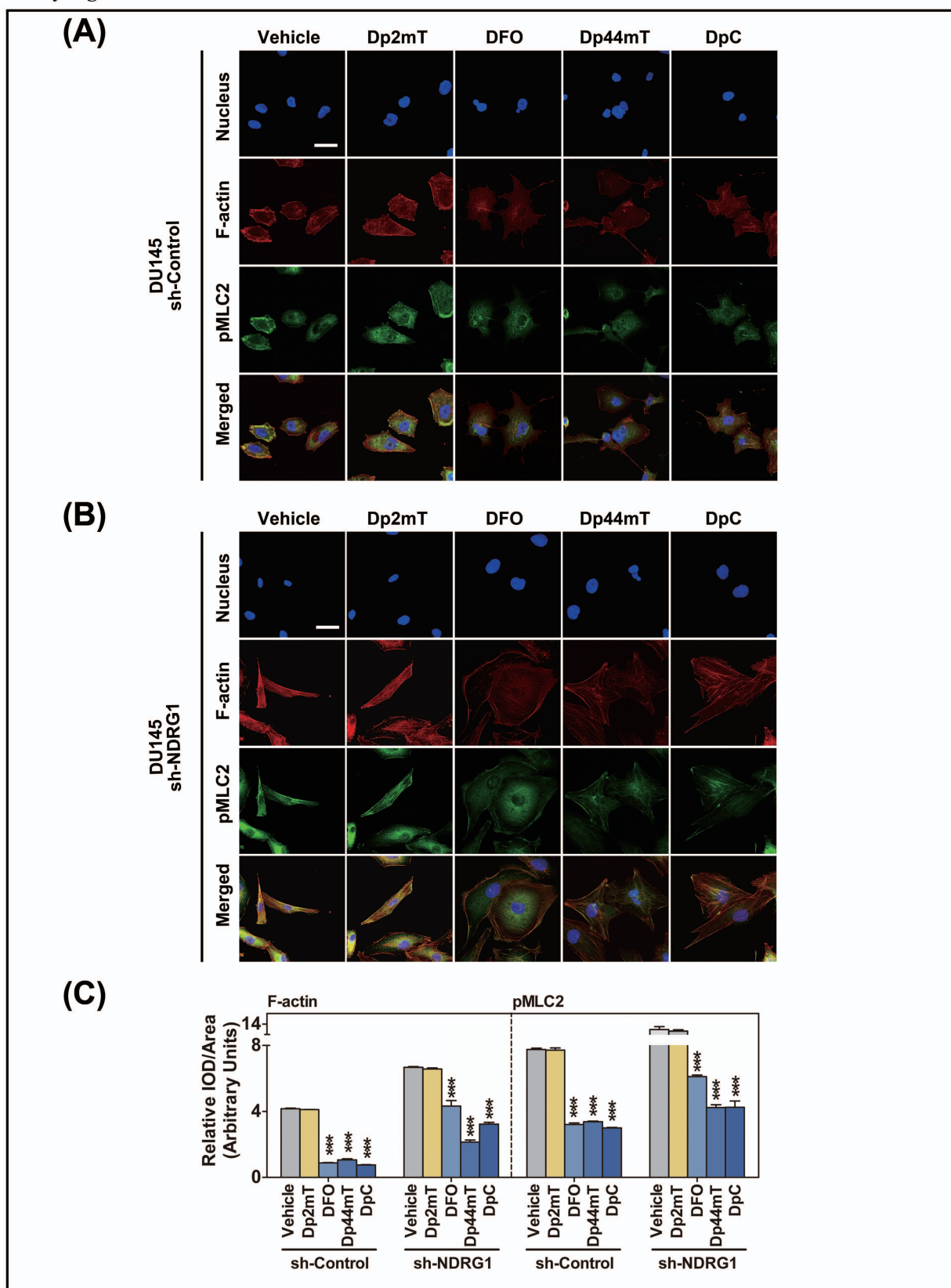
Supplementary Figure 3. The ROCK1 inhibitor, Y27632, inhibits MLC2 phosphorylation and stress fiber formation in DU145, HT29, and HCT116 cells. (A-C) The sh-NDRG1 cells as well as the relative sh-Control cells in the DU145, HT29 and HCT116 cell lines were incubated with the ROCK1 inhibitor, Y27632 (2.5 μ M) for 48 h. Merged immunofluorescence images demonstrate F-actin (red) stained with rhodamine phalloidin, pMLC2 (green) stained with Alexa Fluor[®] 488 and the cell nucleus (blue) stained with DAPI. Scale bars: 25 μ m. (D) Fluorescence quantification was performed by comparing the integrated optical density (IOD)/Area value of F-actin and pMLC2 to the IOD/Area value of nucleus (DAPI) in the same image. Results are typical of 3-5 images from different visual fields and the histogram values are mean \pm SD (3-5 images). *** $p < 0.001$, relative to the respective control cells.

Targeting the Metastasis Suppressor, NDRG1, Using Novel Iron Chelators: Regulation of Stress Fiber-Mediated Tumor Cell Migration via Modulation of the ROCK1/pMLC2 Signaling Pathway

Jing Sun , Daohai Zhang , Ying Zheng, Qian Zhao, Minhua Zheng , Zaklina Kovacevic and Des R. Richardson

Molecular Pharmacology

Supplementary Figure 4



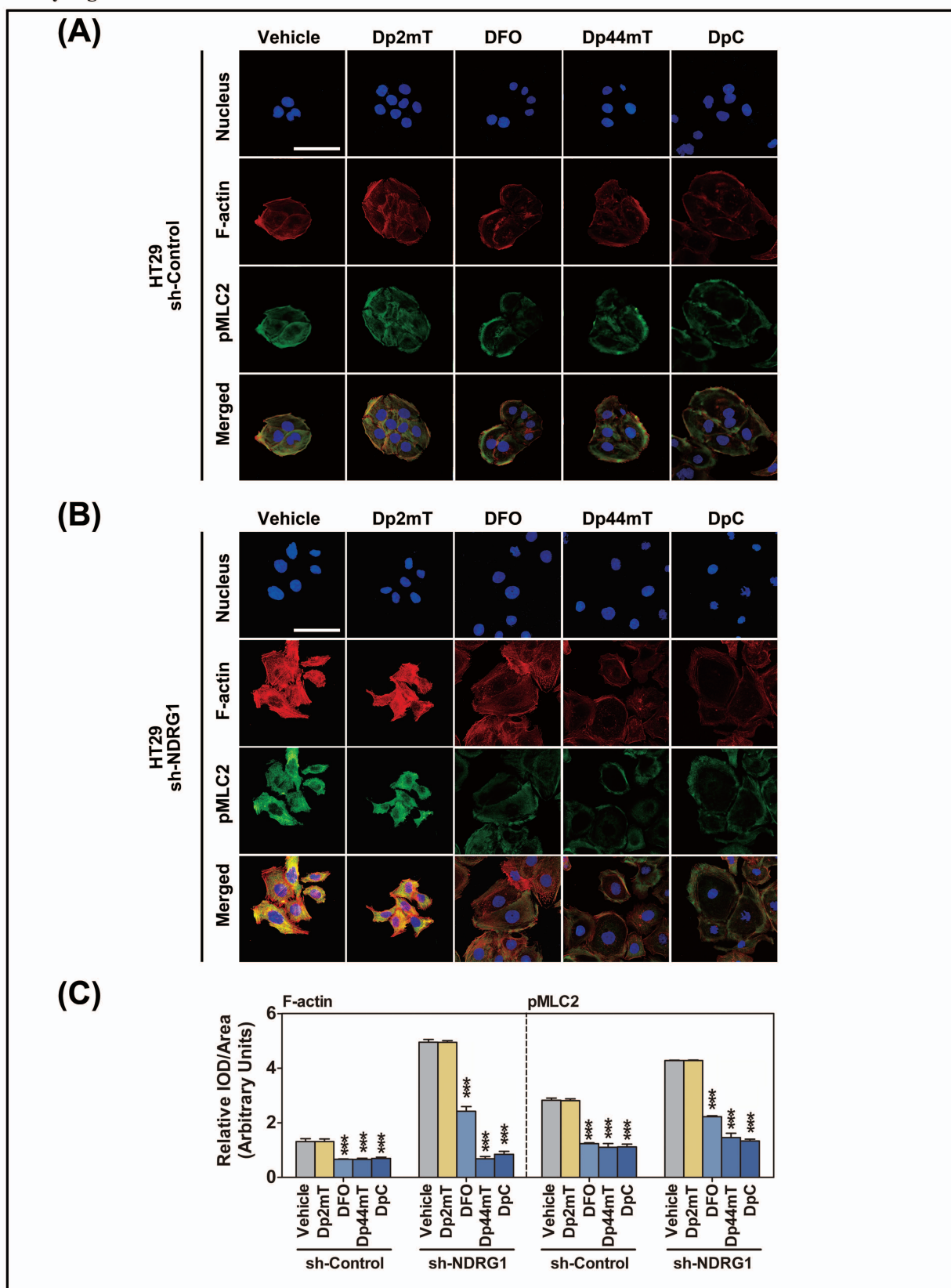
Supplementary Figure 4. Iron chelators inhibit stress fiber assembly and MLC2 phosphorylation in DU145 cells. (A) The DU145 sh-Control cells and (B) DU145 sh-NDRG1 cells were incubated with either: Vehicle control (0.1% DMSO/medium), Dp2mT (10 μ M), DFO (100 μ M), Dp44mT (10 μ M) or DpC (10 μ M) for 24 h. Incubation of both sh-NDRG1 and sh-Control cells with chelators showed an enlarged, epithelial-like phenotype. Moreover, stress fibers as assessed by F-actin staining were less evident in chelator-treated cells relative to those treated with Vehicle or Dp2mT. Scale Bar: 25 μ m. (C) Fluorescence quantification of both F-actin and pMLC2 expression showed an inhibitory effect after incubation with iron chelators. Results in (A) and (B) are typical of 3 experiments, while the densitometry is mean \pm SD (3 experiments). *** $p < 0.001$, relative to cells incubated with the Vehicle or Dp2mT.

Targeting the Metastasis Suppressor, NDRG1, Using Novel Iron Chelators: Regulation of Stress Fiber-Mediated Tumor Cell Migration via Modulation of the ROCK1/pMLC2 Signaling Pathway

Jing Sun , Daohai Zhang , Ying Zheng, Qian Zhao, Minhua Zheng , Zaklina Kovacevic and Des R. Richardson

Molecular Pharmacology

Supplementary Figure 5



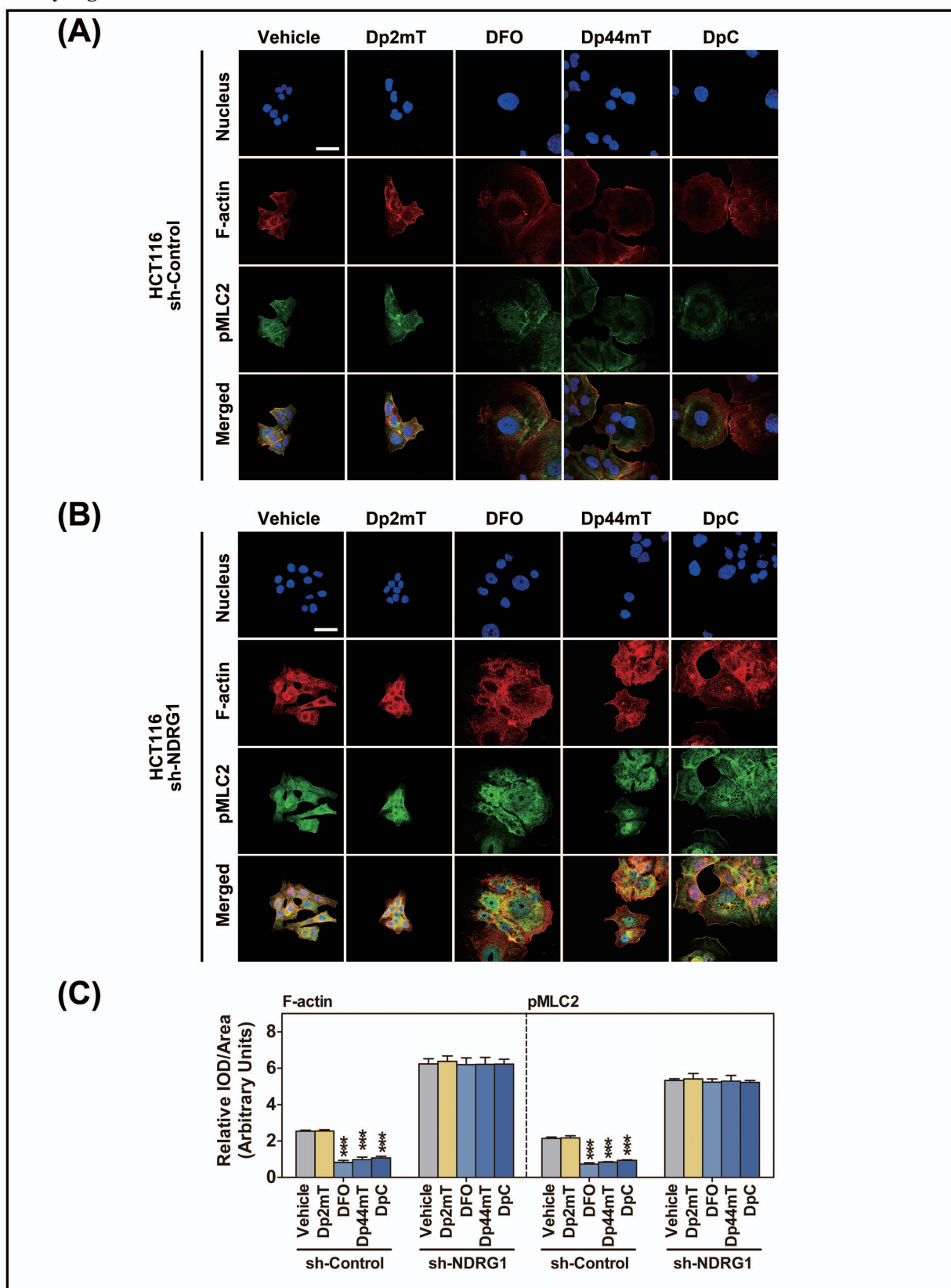
Supplementary Figure 5. Iron chelators inhibit stress fiber assembly and MLC2 phosphorylation in HT29 cells. (A) The HT29 sh-Control cells and (B) HT29 sh-NDRG1 cells were incubated as described in the legend of Supplementary Figure 4. Incubation of sh-NDRG1 and sh-Control cells with chelators resulted in an enlarged, epithelial-like phenotype. Moreover, stress fibers were less evident in chelator-treated cells relative to those treated with the Vehicle or Dp2mT. The staining of F-actin and pMLC2 were re-localized to a cortical location at the cell membrane after incubation of sh-NDRG1 cells with chelators. Scale Bar: 25 μ m. (C) Fluorescence quantification for both F-actin and pMLC2 expression showed an inhibitory effect of chelator treatment. Results in (A) and (B) are typical of 3 experiments, while the densitometry is mean \pm SD (3 experiments). *** $p < 0.001$, relative to cells incubated with the Vehicle or Dp2mT.

Targeting the Metastasis Suppressor, NDRG1, Using Novel Iron Chelators: Regulation of Stress Fiber-Mediated Tumor Cell Migration via Modulation of the ROCK1/pMLC2 Signaling Pathway

Jing Sun , Daohai Zhang , Ying Zheng, Qian Zhao, Minhua Zheng , Zaklina Kovacevic and Des R. Richardson

Molecular Pharmacology

Supplementary Figure 6



Supplementary Figure 6. Iron chelators inhibit stress fiber assembly and MLC2 phosphorylation in HCT116 cells. (A-B) The HCT116 sh-NDRG1 as well as sh-Control cells were incubated as described in the legend of Supplementary Figure 4. After incubation with chelators, both sh-NDRG1 cells and sh-Control cells showed an enlarged, epithelial-like phenotype. Examining sh-Control cells, incubation with chelators reduced the fluorescent staining of both F-actin and pMLC2. In contrast, this did not occur in the sh-NDRG1 cells probably due to the inefficient chelator-mediated up-regulation of NDRG1 in these cells (see Figure 9C). Scale Bar: 25 μ m. (C) Fluorescence quantification of both F-actin and pMLC2 expression showed an inhibitory effect of chelator treatment in sh-Control cells. Results in (A) and (B) are typical of 3 experiments, while the densitometry represents mean \pm SD (3 experiments). *** $p < 0.001$, relative to cells incubated with the Vehicle or Dp2mT.